Cholesterol Modulates Interaction between an Amphipathic Class A Peptide, Ac-18A-NH_2, and Phosphatidylcholine Bilayers†

Masashi Egashira,‡ Galyna Gorbenko,# Masafumi Tanaka,‡ Hiroyuki Saito,|| Julian Molotkovsky,⊥ Minoru Nakano,‡ and Tetsurou Handa*,‡

Graduate School of Pharmaceutical Sciences, Kyoto University, Sakyo-ku, Kyoto 606-8501, Japan, Kharkov National University, 4 Svoboda Square, Kharkov, 61077, Ukraine, Osaka Branch, National Institute of Health Sciences, Osaka 540-0006, Japan, and Shemyakin-Ovchinnikov Institute of Bioorganic Chemistry, Russian Academy of Sciences, 16/10 Miklukho-Maklaya, Moscow, 117871, Russia

Received October 3, 2001

ABSTRACT: Cholesterol (Chol) in phosphatidylcholine large unilamellar vesicles (PC LUV) modulated interaction of the bilayers with a class A amphipathic peptide, Ac-18A-NH_2: Chol increased the peptide binding capacity and reduced the affinity together with the peptide-induced leakage of calcein from LUV. Similar effects of Chol have been observed on the interaction of LUV with apoA-I [Saito, H., Miyako, Y., Handa, T., and Miyajima, K. (1997) *J. Lipid Res. 38*, 287−294]. Circular dichroism (CD) spectra of the peptide indicated a similar helical structure formation in LUV with and without Chol. The fluorescence spectral shift, quantum yield, anisotropy, and acrylamide-quenching of the peptide Trp indicated that in PC:Chol (3:2) LUV, Ac-18A-NH_2 was located in a more polar membrane environment with increased motional freedom and greater accessibility to the aqueous medium. Fluorescence energy transfer from the Trp indole ring to acceptors situated at different depths in the bilayers revealed that the amphipathic peptide penetrated the hydrophobic interior of PC bilayers, while the peptide was located at the polar zwitterionic surface in PC:Chol LUV. The inclusion of Chol causes the headgroup separation of PC at the surface of LUV and increases the binding maximum of the wedge-shaped amphipathic peptide without disrupting the membrane structure. In addition, the rigidifying effect of Chol on PC acyl chains prevents the penetration of the peptide into the bilayer interior. These findings imply that Chol in membranes affects the binding and motional freedom of exchangeable plasma apolipoproteins containing class A amphipathic sequences, e.g., apoA-I and apoCs.

The interaction of exchangeable apolipoproteins with cellular membranes and lipoprotein particles is governed by a wide variety of factors, one of which involves physiologically significant variations in the cholesterol (Chol)[1] content (*1*, *2*). In particular, the level of cellular Chol is found to influence the association of apoA-I and apoE with cultured cells leading to the lipid efflux (*3*−*5*). Several lines of evidence suggest that Chol regulates the metabolism of the lipoproteins and lipid emulsions (*6*, *7*). The modulating effect of Chol is assumed to originate from its ability to change the binding behavior of the apolipoproteins through alterations in the structural state of the lipids and the protein conformation (*8*, *9*). As shown previously, an abundance of Chol in emulsion particles markedly reduces the binding of apoC−II (*10*) and apoA-I to the surface monolayer (*11*, *12*), whereas the incorporation of Chol into the bilayer of lipid vesicles results in a greater binding capacity of apoA-I coupled with a reduced binding affinity (*11*, *12*). These effects are interpreted to mean that the Chol-induced increase in the separation of headgroups leads to a shallower location for apoA-I (*13*).

The lipid-binding domain of apoA-I and other exchangeable apolipoproteins has long been postulated to contain class A amphipathic α-helices having high lipid affinity (*14*). Because of the crucial role of such structural elements in the formation of apolipoprotein−lipid complexes, one approach to gaining insight into the molecular mechanisms of this process involves the examination of model systems containing lipid vesicles or emulsion particles and the class A peptides (*15*−*19*). Despite extensive study of these systems, several important aspects of the problem remain poorly understood. One concerns the effect of Chol on the lipid-associating properties of the class A amphipathic α-helix.

† This work was supported in part by Grants-in-Aid for Scientific Research RC30026103 (to G.G.), 10771274, 12771387 (to H.S.) and 12470488, 12470489 (to T.H.) from JSPS, and grants from the Human Science Foundation of Japan and from the Naito Foundation.

* Address correspondence to Graduate School of Pharmaceutical Science, Kyoto University, Sakyo-ku, Kyoto 606-8501, Japan. Tel: +81-75-753-4555. Fax: +81-75-753-4601. E-mail: handatsr@pharm.kyoto-u.ac.jp.

‡ Kyoto University.

Kharkov National University.

|| National Institute of Health Sciences.

⊥ Russian Academy of Sciences.

[1] Abbreviations: Chol, cholesterol; PC, egg yolk phosphatidylcholine; LUV, large unilamellar vesicles; Ac-18A-NH_2, class A amphipathic peptide (Ac-DWLKAFYDKVAEKLKEAF-NH_2); apoA-I, apolipoprotein A-I; apoCs, apolipoproteins C; apoE, apolipoprotein E; CD, circular dichroism; MBA, 3-methoxybenzanthrone; AV-PC, 1-acyl-2-[12-(9-anthryl)-11-trans-dodecenoyl]-*sn*-glycerophosphocholine; RET, fluorescence resonance energy transfer.

10.1021/bi011885+ CCC: $22.00 © 2002 American Chemical Society
Published on Web 03/03/2002

The present study was undertaken to elucidate the peculiarities in the influence of Chol on the interaction of the model peptide Ac-18A-NH_2 (Ac-DWLKAFYDKVAEK-LKEAF-NH_2) with the lipid bilayers: effects of Chol on binding behavior, leakage activity, structure, and location of the peptide in the bilayers on the basis of CD and fluorescence spectral and resonance energy transfer measurements. Ac-18A-NH_2 is an 18-residue peptide mimicing α-helical segments of exchangeable apolipoproteins, especially apoA-I (*20, 21*).

MATERIALS AND METHODS

Chemicals. Egg yolk phosphatidylcholine (PC) was kindly provided by Asahi Kasei Co. (Japan) and stored in nitrogen atmosphere at −20 °C. The purity, assessed by thin-layer chromatography, exceeded 99.5%. 3-Methoxybenzanthrone (MBA) was purchased from Zonde (Latvia). Anthrylvinyl-labeled phosphatidylcholine, AV-PC (1-acyl-2-[12-(9- anthryl)-11-trans-dodecenoyl]-*sn*-glycerophosphocholine, 1-acyl: 16:0/18:0 = 3/1) was synthesized from egg lysoPC and the fluorescent fatty acid as described in detail elsewhere (*22*). Ac-18A-NH_2 was purchased from Takara Shuzo Co., LTD (Japan). High performance liquid chromatography, amino acid analysis, and mass-spectrometry indicated a peptide purity above 98%. All other chemicals were of special grade from Wako Pure Chemicals (Japan).

Preparation of Lipid Vesicles. LUV were prepared either from PC or a PC:Chol mixture (3:2, mol:mol) by the extrusion method. A thin film obtained by evaporating the lipid chloroform solution was left under vacuum overnight to remove residual organic solvent, and was subsequently hydrated with 10 mM Tris-HCl buffer, pH 7.4, containing 1 mM EDTA. After five rounds of freeze−thawing, lipid suspension was extruded through a 100-nm pore size polycarbonate filter. The phospholipid concentration was determined according to the procedure of Bartlett (*23*). The LUV employed in the resonance energy transfer experiments were prepared by adding AV-PC (0.3−1.5 mol %) or MBA (0.3−1.3 mol %) to the lipid chloroform solution, followed by vacuum-drying, hydration, freeze−thawing, and extrusion. Concentrations of AV-PC and MBA in model membranes were determined spectrophotometrically, after diluting the vesicle suspension 10-fold with ethanol, using extinction coefficients $E_{367} = 9 \times 10^3\ M^{-1}\ cm^{-1}$ (AV-PC) (*22*) and $E_{420} = 9.6 \times 10^3\ M^{-1}\ cm^{-1}$ (MBA) (*24*). All measurements were completed within 12 h after LUV preparation.

Ac-18A-NH_2 Binding Assays. Mixtures (500 μL) of a constant amount of LUV (1−5 mM for PC) and various amounts of Ac-18A-NH_2 were incubated for 1 h to equilibrate the free and bound peptides at 25 °C. After addition of 3% sucrose to adjust the density, each mixture was ultracentrifuged to separate the bound (the top fraction) from free peptide (the bottom fraction, 200 μL). The centrifugation period of 1 h was selected to give stationary values of bound peptide. The bottom fractions were collected, and then 100 μL of 10% nonionic surfactant, heptaethyleneglycolmonododecyl ether, was added (*11, 13*). These samples were left overnight at 4 °C to solubilize the small amounts of remaining lipid. The peptide concentration in the fraction was determined by measuring the peak area of Trp fluorescence near 335 nm (excitation at 280 nm). The lipid-bound peptide amount was calculated from the difference between the peptide concentrations before and after ultracentrifugation. Binding data were analyzed according to the following equation:

$$\frac{P_b}{[PC]} = N\frac{P_f}{(K_d + P_f)} \quad (1)$$

where, P_f and P_b are the free and bound peptide concentrations (μM), respectively, [PC] is the concentration of PC at outer leaflets of vesicles (mM), N is the binding maximum (mmol of Ac-18A-NH_2/mol of PC), and K_d is the dissociation constant (μM). [PC] was determined by a ^{31}P-NMR method with a bilayer-impermeable paramagnetic ion (*10*).

Fluorescence Leakage Assay. For leakage measurements, a fluorescence dye, calcein (Dojindo), was entrapped in LUV. The dried lipid film was hydrated with 70 mM calcein. After extrusion of the lipid, untrapped dye was removed by gel filtration through a Bio-Rad A-50 m column eluted with the buffer. An AC-18A-NH_2 solution was added to the calcein-entrapped LUV at 25 °C. Fluorescence intensity was measured at 520 nm (excitation at 490 nm). The percent leakage of calcein at 1 h was determined using the fluorescence intensity corresponding to 100% leakage obtained in the presence of 0.3% Triton X-100 (*11*). The peptide/PC mole ratio was less than 0.01, and disintegration or solubilization of LUV was not observed.

CD Spectral Measurements. CD spectra were recorded from 195 to 250 nm with a JASCO J-720 spectropolarimeter at 25 °C. A 0.1-cm path-length cell was used to obtain the peptide spectra at 10 μM. The PC concentration of LUV was varied to obtain stationary spectra at 1 mM. The mean-residue ellipticity at 222 nm was used for estimation of the percent helicity of the peptide (*25*).

Fluorescence Measurements. Fluorescence measurements were performed with a HITACHI F-4500 spectrofluorimeter using a 5-mm path-length cuvette. Peptide emission spectra were recorded at 25 °C with excitation at 296 nm. Excitation and emission slit widths were set at 5 nm. In the quenching and resonance energy transfer experiments, the measured fluorescence intensities were corrected for the inner filter and reabsorption effects (*26*).

Fluorescence quenching experiments were carried out using a neutral water soluble quencher, acrylamide. Small aliquots (10 μL) of acrylamide stock solution (2 M) were added to a constantly stirred and temperature-controlled solution (0.4 mL) of the peptide or peptide-lipid mixture. The data for the quenching experiments were analyzed according to the Stern−Volmer equation (*27*):

$$\frac{F_o}{F_q} = 1 + K_{SV}[Q] = 1 + k_q\tau_o[Q] \quad (2)$$

where F_o and F_q are the peptide fluorescence intensities in the absence and presence of the quencher, respectively, [Q] is the quencher concentration, K_{SV} is the Stern−Volmer constant, k_q is the bimolecular rate constant, and τ_o is the fluorescence lifetime.

The efficiency of the resonance energy transfer between the peptide tryptophan as donor and AV-PC or MBA as acceptors was determined by estimating the ratio of the Trp

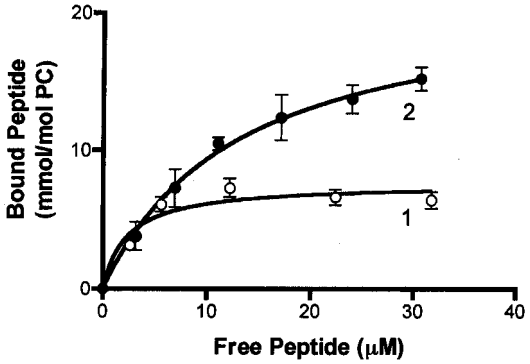

FIGURE 1: Binding profiles of Ac-18A-NH_2 in PC LUV (1) and PC:Chol (3:2) LUV (2). Each point represents the mean of five experiments at 25 °C. The solid lines are theoretical curves calculated using K_d and N values listed in Table 1.

quantum yields in the presence of acceptor-containing and acceptor-free vesicles. The critical distance of energy transfer (Förster radius, nm) was calculated as (*27*):

$$R_o = 979(\kappa^2 n_r^{-4} Q_d J)^{1/6} \quad (3)$$

$$J = \frac{\int_0^\infty F_D(\lambda)\epsilon_A(\lambda)\lambda^4 d\lambda}{\int_0^\infty F_D(\lambda) d\lambda} \quad (4)$$

where Q_d is the donor quantum yield, n_r is the refractive index of the medium ($n_r = 1.37$), κ^2 is an orientation factor, J is the overlap integral determined by numerical integration, $F_D(\lambda)$ is the donor fluorescence intensity, and $\epsilon_A(\lambda)$ is the acceptor molar absorbance at the definite wavelength λ. For the donor−acceptor pair of Trp and AV-PC, R_o values were found to be 2.23 nm (PC LUV) and 2.26 nm (PC:Chol LUV), while for the pair of Trp and MBA, R_o values were 1.88 nm (PC LUV) and 1.95 nm (PC:Chol LUV). Here, the dynamically averaged value of κ^2, 0.67, was used in eq 3. The anisotropy, quenching, and energy transfer measurements of the lipid-bound peptide were performed under conditions where the fraction of free peptide recovered from the control binding experiments does not exceed 6%. Slight light scattering due to LUV was subtracted from the fluorescence intensities of the peptide in these measurements.

RESULTS

Binding of Ac-18A-NH_2 to LUV. Figure 1 shows the binding profiles of Ac-18A-NH_2 to PC and PC:Chol LUV. The amount of bound Ac-18A-NH_2 increased with the peptide concentration. The data fitting procedure using eq 1 gave the binding maximum, N and the dissociation constant, K_d (Table 1). The inclusion of Chol in PC bilayers decreased the affinity, ($1/K_d$) of the peptide to 15%, while the N value increased to 3 times the value in PC LUV. The area per Ac-18A-NH_2 molecule was 85.8 nm^2 at the PC LUV surface and 35.1 nm^2 at the PC:Chol LUV surface (see in Appendix). Similar effects of Chol have been observed in the sparse binding of apoA-1 to LUV (*11*−*13*).

Leakage of Calcein from LUV. In the absence of the peptide, no leakage of calcein was observed in either PC or PC:Chol LUV. The leakage was evaluated at 10 μM Ac-18A-NH_2 in LUV of 1 mM PC (Figure 2). While PC and PC:Chol LUV had similar amounts of bound peptide per mole of PC at this peptide/LUV ratio (about 5 mmol/mol of PC, see Figure 1), much less Ac-18A-NH_2 leaked out in PC:Chol LUV than in PC LUV: 15 and 4% leakage in 2 h, respectively. The leakage from LUV did not accompany any change in the hydrodynamic radius. An analogous inhibitory effect of Chol on the leaking of apoA-I has been reported in LUV (*11*).

Table 1: Binding Parameters of Ac-18A-NH_2 in PC and PC:Chol LUV

	PC LUV	PC:Chol LUV (3:2)
K_d (μM)	2.28 ± 1.30	13.1 ± 1.32
N (mmol of peptide/mol of PC)	7.57 ± 0.88	21.6 ± 0.93
PC/peptide (mol/mol)	132	46
(PC + Chol)/peptide (mol/mol)	132	77
area in nm^2/peptide[a]	85.8	35.1

[a] In PC LUV, the molecular area of PC is 0.65 nm^2 (*48*), and in PC:Chol LUV, the molecular areas of PC and Chol are 0.5 and 0.39 nm^2 (*59*), respectively.

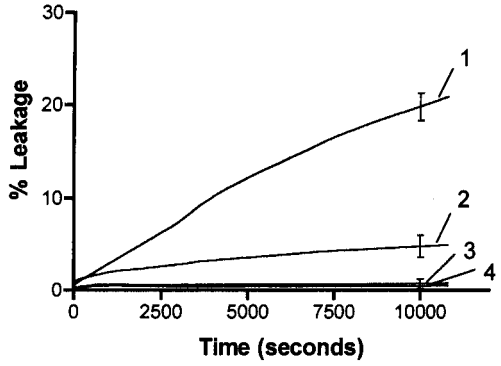

FIGURE 2: Ac-18A-NH_2 induced leakage of calcein from PC and PC:Chol (3:2) LUV. LUV of 1 mM PC were incubated in the presence of 10 μM Ac-18A-NH_2 at 25 °C. 1:PC LUV + Ac-18A-NH_2, 2:PC:Chol (3:2) LUV + Ac-18A-NH_2, 3 and 4: PC and PC:Chol LUV without the peptide.

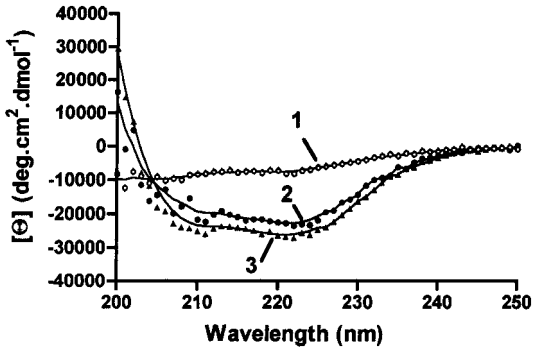

FIGURE 3: CD spectra of Ac-18A-NH_2 in buffer, PC and PC:Chol LUV. 1: in buffer (α-helix content:11%), 2: in PC:Chol (3:2) LUV (68%), 3: in PC LUV (77%). Peptide and PC concentrations were 10 μM and 1 mM, respectively.

α-*Helical Content.* The CD results showed that the α-helical content of the peptide (10 μM) increased upon interaction with LUV bilayers. The helicity became stationary at the PC concentration of 1 mM. The α-helical contents were 11, 77, and 68% in the aqueous medium, PC, and PC:Chol LUV, respectively (Figure 3). The value in PC LUV was comparable with that in POPC LUV of 100 nm (71%) (*28*) and in DMPC bilayers (72%) (*21*). Therefore, irrespective of the presence of Chol, the peptide interaction

Table 2: Fluorescence Characteristics of Ac-18A-NH_2 Trp in Solution and in the Lipid-Bound State

fluorescence parameter	in buffer[a]	in PC LUV	in PC:Chol (3:2) LUV
emission max (nm)	349 ± 3	333 ± 2	345 ± 2
quantum yield (relative to free Trp in water[b])	0.52 ± 0.04	0.93 ± 0.05	0.78 ± 0.05
anisotropy	0.09 ± 0.004	0.16 ± 0.004	0.06 ± 0.006
Stern−Volmer constant for acrylamide quenching (M^{-1})	5.1 ± 0.7	0.2 ± 0.03	1.2 ± 0.2

[a] 10 mM Tris-HCl, 1 mM EDTA, pH 7.4. [b] Quantum yield of Trp in water was taken to be 0.14 [Kirby, E., and Steiner, R. (1970) *J. Phys. Chem. 74*, 4480−4490].

with LUV brought about a pronounced increase in the helicity.

Fluorescence Spectral Changes. The data summarized in Table 2 show that in buffer solution, this peptide had an emission maximum at 349 nm, characteristic of Trp (W) in an aqueous environment (*29*). The quantum yield of the Ac-18A-NH_2 Trp equaled 52% of that for a free Trp in water. Peptide binding to PC vesicles resulted in a pronounced blue shift of the emission maximum (ca. 16 nm) coupled with an increase in the Trp quantum yield by 79% as compared to that in the buffer. Such spectral changes are generally explained by the transfer of fluorophore into a less polar and/or motionally more restricted environment (*30, 31*). Effects similar in character, but substantially less in magnitude, were observed on the interaction of Ac-18A-NH_2 with the lipid vesicles containing 40 mol % Chol. In this case, the shift in the emission maximum was found not to exceed 4 nm. Peptide partitioning into PC:Chol bilayers led to less of an increase in the Trp quantum yield (ca. 50%) than that for PC bilayers.

The interaction of peptide with PC LUV was followed by monitoring the increase in Trp fluorescence anisotropy indicating a reduction in the rotational mobility of Trp. By contrast, in the PC:Chol LUV, the mobility appeared to be similar to or greater than that in buffer solution (Table 2).

Fluorescence Quenching. As can be seen in Figure 4 and Table 2, the binding of Ac-18A-NH_2 to LUV was followed by a decrease in the Stern−Volmer constant for acrylamide quenching. The effect was much more pronounced for PC LUV. Since acrylamide is a water-soluble quencher and shown not to penetrate the hydrophobic region of PC bilayer (*27*), the observed changes could be interpreted as a reduction in the accessibility of Trp to the solvent. However, the results of the quenching experiments indicate that other factors may contribute to the decrease of K_{sv}. The first one is the reduced bimolecular rate constant for collisional quenching due to the slower translational diffusion of the Trp residue immobilized on the surface of lipid vesicles. The possible contribution of this phenomenon to the K_{sv} decrease can be approximately assessed by calculating the ratio of the k_q values in eq 2 according to the Smoluchowski equation (*32*). The slower translational diffusion of the peptide−lipid complex was estimated to decrease the K_{sv} value by a factor of ca. 2.9. The magnitude of the observed changes in K_{sv} (a

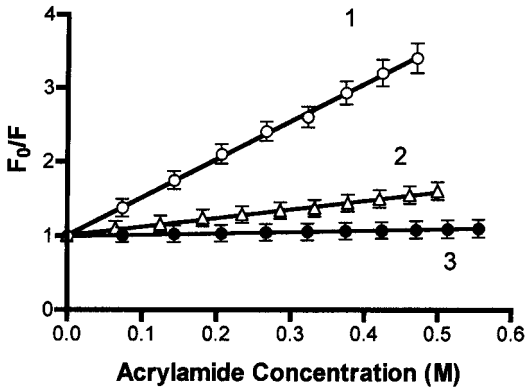

FIGURE 4: Stern−Volmer plots for the fluorescence quenching of Ac-18A-NH_2 by acrylamide. 1: in buffer; 2: in PC:Chol (3:2) LUV, 3: in PC LUV. Lipid/peptide molar ratio: 310/1 (PC), 850/1 (PC:Chol). The measurements for the lipid-bound peptide were performed under conditions where the fraction of free peptide does not exceed 6%. Stern−Volmer constant; see Table 2.

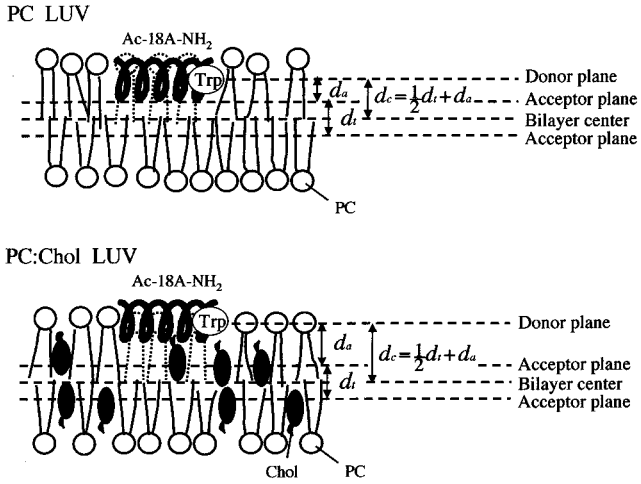

FIGURE 5: Schematic representation of the donor (Ac-18A-NH_2 Trp) and acceptor locations in LUV. Upper: PC LUV; lower: PC:Chol (3:2) LUV. The Trp distances from the bilayer center, d_c, were evaluated as ca. 1 and 2 nm in PC and PC:Chol LUV, respectively (see eq 7 in the text).

26- and 4-fold decrease for PC and PC:Chol LUV, respectively) exceeds the aforementioned estimate, suggesting a reduction of the peptide Trp on exposure to the solvent. The second factor is the effect of change in lifetime of the peptide Trp. However, Table 2 shows that variation in the quantum yield (i.e., lifetime) between PC and PC:Chol bilayers is very small as compared with that in the K_{sv} value.

Location of Trp as Revealed by Resonance Energy Transfer (RET). To derive quantitative estimates characterizing the position of Ac-18A-NH_2 Trp in the lipid bilayer, the results of RET measurements were analyzed in terms of the modified model of Wolber & Hudson developed for the case of donors and acceptors randomly distributed on a planar surface (*33*). In the present study, we extended this model assuming that there exist one donor plane situated in the outer monolayer and two acceptor planes residing in the outer and inner membrane leaflets (Figure 5). The validity of such an assumption is confirmed by the available information on the location of the donor (Ac-18A-NH_2 Trp), and the acceptors (MBA and the anthrylvinyl fluorophore of AV-PC) in the lipid bilayers. As was demonstrated in recent studies, the amphipathic helix of Ac-18A-NH_2 resides at the interfacial

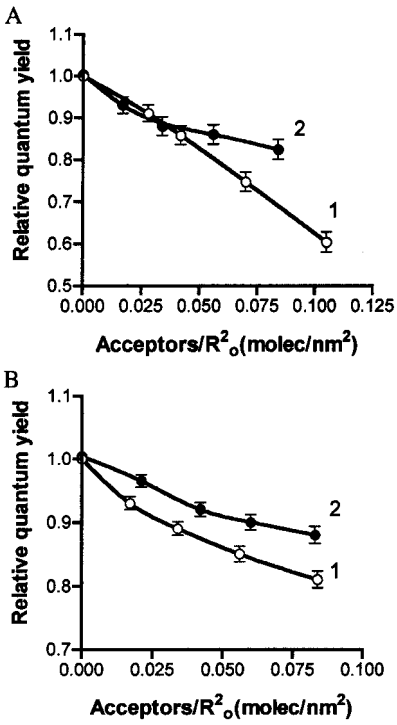

FIGURE 6: Relative quantum yield of the donor, Ac-18A-NH_2 Trp as a function of surface acceptor concentration (molec/R_0^2). (A) acceptor AV-PC, 1 in PC LUV ($R_0 = 2.23$ nm), 2 in PC:Chol LUV ($R_0 = 2.25$ nm); (B) acceptor MBA, 1 in PC LUV ($R_0 = 1.88$ nm), 2 in PC:Chol LUV ($R_0 = 1.95$ nm). Here, κ^2 in eq 3 is assumed as 0.67.

region of the outer monolayer adopting a parallel orientation to the membrane surface (*34*, *35*). The neutral hydrophobic probe MBA is thought to be localized at the boundary of polar and nonpolar membrane areas in the vicinity of the glycerol moiety (*36*), while the anthrylvinyl fluorophore of AV-PC is situated among the terminal methyl groups of the lipid acyl chains (*22*).

Relative quantum yield of the donor (Q_r) can be represented as:

$$Q_r = Q_{DA}/Q_D \tag{5}$$

where Q_D and Q_{DA} are the donor quantum yields in the absence and presence of acceptor, respectively. Figure 6 shows relative quantum yield of the donor as a function of surface acceptor concentration. RET efficiencies from Ac-18A-NH_2 Trp to AV-PC (A) and to MBA (B) are higher in PC LUV than in PC:Chol LUV. To determine the Trp position in the lipid bilayers, experimental Q_r values (Q_r^e) were fitted to the theoretical values (Q_r^t) predicted by the above model (in Appendix and Figure 5). The fitting procedure involved the minimization of the function:

$$f = \frac{1}{n_a}\sum_{i=1}^{n_a}(Q_r^e - Q_r^t)^2 \tag{6}$$

where Q_r^t is a function of the distance between two separating acceptor planes d_t, separation of the donor and the nearest acceptor planes d_a and the orientation factor κ^2 as presented in Figure 5 (also refer to Appendix); n_a is the number of Q_r values measured at the various acceptor concentrations.

During the data fitting, parameters d_t and κ^2 were held constant, while parameter d_a was optimized. The value of d_t was slightly varied in the limits consistent with the putative membrane location of the acceptor planes (0.2−0.3 nm for AV-PC and 2.4−2.6 nm for MBA). Chol in bilayers expels other bulky groups from the region at the level of glycerol residue and upper methylene groups of PC acyl chain. But the AV group of AV-PC is located at the center of bilayers (*37*), in the region that is reached only by Chol tails, and it is presumed that Chol in bilayers does not significantly affect the location of the AV fluorophore. The unambiguous choice of the κ^2 value appeared to be more problematic because any accurate experimental or theoretical estimation of this parameter for the fluorophores localized in the lipid bilayers is impossible. It is the most common approach in the RET studies to put κ^2 equal to 0.67, the dynamically averaged isotropic value, valid for the random reorientation of the donor emission and acceptor absorption transition dipoles. However, in the present work we could not follow this approach since anisotropy measurements suggested restricted mobility of the donors and acceptors in the membrane interior. In view of this, in analyzing experimental data, it seemed reasonable to vary the κ^2 value over the widest theoretical limits: from 0 to 4 (*27*). Ultimately, we obtained sets of parameters (d_a, d_t, κ^2) corresponding to the minimum of the fit function (*6*). These data were used subsequently in calculating the distance of Trp from the bilayer center (d_c):

$$d_c = 0.5d_t \pm d_a \tag{7}$$

where "+" accounts for the case when acceptors in the outer monolayer reside closer to the bilayer center than donors, and "−" for the opposite case. Minimization of the fit function yields the relation between the d_c value and orientation factor κ^2 as seen in Figure 7.

DISCUSSION

Binding of Ac-18A-NH_2 and Leakage of Calcein from LUV. The helix of the class A peptide has been suggested to have a wedge-shaped cross section, which favors the highly curved structure of high-density lipoproteins (*21*). The peptide bound to the planar PC bilayers creates local defects in LUV and causes a rather slow leakage of calcein from the vesicles (Figure 2). Despite the leakage, it was confirmed that the peptide binding did not alter the size of LUV under the current experimental conditions. However, when the peptide/PC mole ratio increased to 1/1, PC LUV were rapidly disintegrated to give decreased light scattering as reported previously (*19*). The observation indicates that the helix is inserted into the hydrophobic interior of the bilayers and disturbs the membrane structure. Certain antimicrobial peptides at the bilayer surface fold into amphipathic helices, aggregate, and form multiple pores, leading to leakage from the vesicles (*38*). It is not clear if Ac-18A-NH_2 forms similar pores; however, the interaction between the hydrophobic surface of the amphipathic helix and the nonpolar interior of the bilayers seems to be of primary importance to the leakage of LUV.

The incorporation of Chol into PC LUV caused the PC headgroups to separate (*11*, *13*, *39*−*41*). The interfacial space allowed more peptide binding (46 PC + 31 Chol molecules

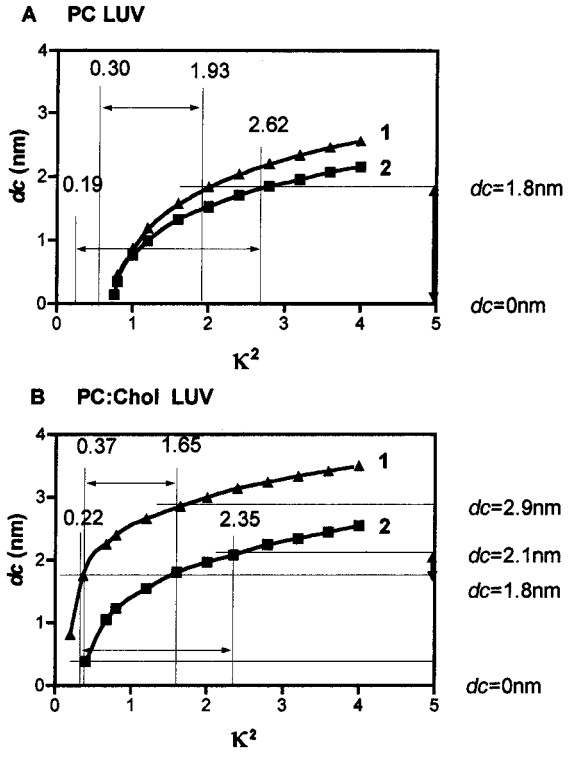

FIGURE 7: The distance of Ac-18A-NH_2 Trp residue from the lipid bilayer center (d_c) as a function of orientation factor (κ^2). (A) PC LUV, (B) PC:Chol (3:2) LUV. Donor: Ac-18A-NH_2, Acceptors 1: MBA, 2: AV-PC. Minimization of the fitting function, eq 6, gives the d_c value as a function of κ^2. The possible d_c boundaries were evaluated for both acceptors (Table 3) and the common limit was determined as the optimal range of the d_c value: $d_c = 0-1.8$ nm in PC LUV; $d_c = 1.8-2.1$ nm in PC Chol LUV. Further narrowing of the d_c value in PC LUV (ca. 1 nm) was based on the relationship between the emission maximum of Trp and the position within the membrane (*46*).

or 35.1 nm^2 per Ac-18A-NH_2 for PC:Chol LUV vs 132 PC molecules or 85.8 nm^2 per Ac-18A-NH_2 for PC LUV) coupled with a lower affinity ($1/K_d = 0.076\ \mu M^{-1}$ for PC:Chol LUV vs $0.438\ \mu M^{-1}$ for PC LUV). The lower affinity and leakage activity suggest that the peptide binds to the PC:Chol bilayers through insertion between the phospholipid headgroups but does not penetrate deeply into the hydrocarbon interior, as compared to PC LUV.

Ac-18A-NH_2 at the Surface of LUV. As shown in Table 2, the binding of Ac-18A-NH_2 to either PC or PC:Chol LUV resulted in an increase in the quantum yield of Trp and a blue shift of the emission maximum. These changes can be attributed to the lowered polarity and decreased motional freedom of the fluorophore surroundings, i.e., the peptide Trp residue is situated much more deeply in the PC bilayers than in the PC:Chol bilayers. This assumption is supported by the quenching experiments indicating enhancement of the accessibility to Trp by the solvent upon the inclusion of Chol (Figure 4 and Table 2) and is compatible with the lower binding affinity and reduced leakage activity of the peptide in PC:Chol LUV.

Further evidence that the depth of penetration of the Trp in bilayers was reduced in the presence of Chol comes from the RET measurements. As seen from the $d_c - \kappa^2$ relationships in Figure 7A, the minimum possible κ^2 value for Ac-18A-NH_2 at the surface of PC LUV (corresponding to $d_c = 0$) is greater than the isotropic value (0.67), suggesting a preferential orientation of the Trp indole ring. This could be a consequence of the restriction of the fluorophore rotational mobility in the lipid-bound peptide and specific orientation of the amphipathic helix relative to the lipid−water interface. The former possibility is corroborated by the high anisotropy value (0.16) observed for Ac-18A-NH_2 bound to PC LUV (Table 2), while the latter is substantiated by the recent X-ray diffraction (*35*) and oriented CD data (*42*) indicating that the Ac-18A-NH_2 helix adopts an orientation parallel to the membrane surface in the DOPC bilayers.

To minimize the uncertainty in the estimation of d_c originating from the unknown κ^2 value, we calculated the lower and upper κ^2 limits using the approach of Dale et al. (*43*). According to this approach, the minimum and maximum κ^2 values are defined as:

$$\kappa_{min}^{\ 2} = 2/3(1 - 0.5(d_D + d_A)) \quad (8)$$

$$\kappa_{max}^{\ 2} = 2/3(1 + d_D + d_A + 3d_D d_A) \quad (9)$$

where d_D and d_A are depolarization factors, related to the steady-state (r) and fundamental anisotropies (r_o) of the donor and acceptor:

$$d_D = \left(\frac{r_D}{r_{oD}}\right)^{1/2}; \quad d_A = \left(\frac{r_A}{r_{oA}}\right)^{1/2} \quad (10)$$

Presented in Table 3 are the orientation factor boundaries calculated from eqs 8−10 for the donor−acceptor pairs. In determining these parameters, we used the peptide Trp, AV-PC, and MBA anisotropies measured in PC and PC:Chol LUV and fundamental anisotropies reported for indole (0.3 at $\lambda_{ex} = 296$ nm (*44*)), AV-PC (0.08 at $\lambda_{ex} = 300$ nm (*45*)), and MBA (0.34 at $\lambda_{ex} = 420$ nm (*36*)). Calculated in such a way, κ^2 limits were employed in estimating the minimum ($d_{c\ min}$) and maximum ($d_{c\ max}$) values of the distance of the peptide Trp from the bilayer center. By combining the data obtained with the two different acceptors, it follows that for the PC bilayer, d_c limits are 0−1.8 nm (including the glycerol moiety, carbonyls, and acyl chain carbons), while for PC:Chol LUV, the d_c value falls in the range 1.8−2.1 nm (corresponding to the location of Trp in the vicinity of the phospholipid zwitterionic group) as seen in Figure 7 and Table 3.

In an attempt to further narrow down the limits of d_c, we took into consideration the relationship between the emission maximum of Trp and the position of fluorophore within the membrane (*46*). For a λ_{max} value of 333 nm (Ac-18A-NH_2 in PC LUV), the analysis gave a d_c value of ca. 1 nm. Given the structural peculiarities of the lipid bilayer (*47*), one can conclude that in PC LUV, the Trp residue is located in the interfacial region comprising the glycerol backbone, carbonyl groups, and upper methylene groups of phospholipid molecules (*48*). Taken together with the d_c for PC:Chol LUV (1.8−2.1 nm), our findings suggest that Chol modifies the character of the peptide−bilayer interactions, causing the amphipathic helix to be less deeply buried in the membrane interior. It has been known that 30−40% Chol in bilayers leads to a change in length of phospholipid hydrophobic tail of 0.2−0.25 nm (*49*, *50*), but much smaller than the variation of Ac-18A-NH_2 Trp position with and without Chol, ca. 1 nm.

Table 3: Orientation Factor Boundaries (κ_{min}^2 and κ_{max}^2)[a] and Corresponding Limiting Values of the Ac-18A-NH_2 Trp Distance from the Bilayer Midplane ($d_{c\ min}$ and $d_{c\ max}$)[b]

	PC LUV		PC:Chol (3:2) LUV	
acceptor	$d_{c\ min}$ (nm)	$d_{c\ max}$ (nm)	$d_{c\ min}$ (nm)	$d_{c\ max}$ (nm)
AV-PC	0 ($\kappa_{min}^2 = 0.19$)	1.8 ($\kappa_{max}^2 = 2.62$)	0 ($\kappa_{min}^2 = 0.22$)	2.1 ($\kappa_{max}^2 = 2.35$)
MBA	0 ($\kappa_{min}^2 = 0.30$)	1.8 ($\kappa_{max}^2 = 1.93$)	1.8 ($\kappa_{min}^2 = 0.37$)	2.9 ($\kappa_{max}^2 = 1.65$)

[a] Orientation factor boundary was determined by using eqs 8−10. [b] Limiting values of d_c were evaluated in Figure 7.

Role of Chol in Class A Peptide−Lipid Interaction. A growing body of evidence shows that Chol-rich domains are present in the membranes of mammalian cells, and Chol has been indicated to play roles in the interaction with apoA-I (*11*) and in Chol efflux from cells (*51*). It is assumed that Chol prevents deep penetration of the bilayer interior by increasing the acyl chain packing density (*52*−*54*). Furthermore, solid state ^{2}H and ^{31}P NMR studies have revealed a mutual compensation for the changes in the intrinsic monolayer curvature caused by melittin and Chol (*55*). The membrane monolayer curvature is believed to be dependent on the depth of the α-helix insertion into the membrane (*56*). The class A amphipathic helices represented by Ac-18A-NH_2 are characterized by a wedge-shaped cross-section (*39*, *40*). This structural feature is responsible for the ability of this kind of helix to promote a positive curvature strain in the membrane monolayer (*41*, *56*). Chol, increasing the separation of phospholipid headgroups and causing tighter packing of the acyl chains, could reduce the depth of Ac-18A-NH_2 penetration in the lipid bilayers and moderate the curvature strain.

Although the CD spectra indicated similar α-helical content of the bound peptide in the two types of LUV (Figure 3), fluorescence anisotropy measurements revealed a considerable difference in the rotational mobility of Trp (Table 2). The shallow insertion of the amphipathic helix in the Chol-containing LUV increased the mobility of the Trp residue near the helix-end.

In this context, it is worth noting that Chol is reportedly capable of altering the conformation of apoA-I (*9*, *57*). It has been found that addition of Chol to reconstituted lipoprotein particles is followed by an increase in the apoA-I net negative charge and decrease in its helix content (*9*). Immunochemical studies have revealed a specific effect of Chol on the tertiary structure of the apoA-I central domain between residues 99 and 143 (*57*). Two explanations for these effects have been proposed: direct interaction of Chol with the protein and modification of the lipid packing influencing the conformation of apoA-I. According to the polarographic data, Chol decreases the extent to which apoA-I penetrates the membrane interior (*58*). Using ^{13}C NMR and fluorescent probes sensitive to changes in phospholipid hydration, we have established a correlation between the apoA-I binding maximum and the headgroup separation of PC in model membranes differing in Chol content (*11*, *13*). Therefore, Chol in PC membranes leads to the concentration of class A peptides and apoA-1 with increased motional freedom and greater accessibility to the medium.

APPENDIX

Relative Quantum Yield in the RET Study (24). Considering two acceptor planes separated by a distance d_t, the relative quantum yield of a donor (Q_r) can be represented as:

$$Q_r = \frac{Q_{DA}}{Q_D} = 0.5\left(\int_0^\infty \exp[-\lambda](I_1(\lambda))^{N_1} d\lambda + \int_0^\infty \exp[-\lambda](I_2(\lambda))^{N_2} d\lambda\right) \quad \text{(A1)}$$

$$I_1(\lambda) = \int_{d_a}^{R_d} \exp[-\lambda(R_o/R)^6]\left(\frac{2R}{R_d^2 - d_a^2}\right) dR \quad \text{(A2)}$$

$$I_2(\lambda) = \int_{d_t \pm d_a}^{R_d} \exp[-\lambda(R_o/R)^6]\left(\frac{2R}{R_d^2 - (d_t \pm d_a)^2}\right) dR \quad \text{(A3)}$$

$$N_1 = \pi C_a^s (R_d^2 - d_a^2) \quad \text{(A4)}$$

$$N_2 = \pi C_a^s (R_d^2 - (d_t \pm d_a)^2) \quad \text{(A5)}$$

where Q_D, Q_{DA} are the donor quantum yields in the absence and presence of acceptor, respectively; $\lambda = t/\tau_d$, τ_d is the lifetime of an excited donor in the absence of acceptor; N is the number of acceptors within the disk of radius R_d, beyond which energy transfer is insignificant; C_a^s is the acceptor concentration per unit area; and d_a is the separation of a donor plane and the nearest acceptor plane. Subscripts "1" and "2" correspond to the outer and inner bilayer leaflets, respectively. The surface acceptor concentration was calculated from:

$$C_a^s = \frac{B_A}{L_o(X_{PC}S_{PC} + X_{Chol}S_{Chol})} \quad \text{(A6)}$$

where B_A and L_o are the molar concentrations of the membrane-bound acceptor (the peptide Trp) and lipid (PC + Chol), respectively; X_{pc} and X_{Chol} are the mole fractions of PC and Chol, and S_{PC} and S_{Chol} are the mean areas per lipid molecule. For the PC bilayer, S_{PC} was taken to be 0.65 nm^2 (*48*), while for the PC:Chol model membrane, the following values were used: $S_{PC} = 0.5$ nm^2, $S_{Chol} = 0.39$ nm^2 (*59*), taking into account the condensation effect of Chol on PC bilayers.

REFERENCES

1. Johnson, W., Mahlberg, F., Rothblat, G., and Phillips, M. (1991) *Biochim. Biophys. Acta 1085*, 273−298.
2. Derksen, A., Gantz, D., and Small, D. (1996) *Biophys. J. 70*, 330−338.
3. Bielicki, J., Johnson, W., Weinberg, R., Glick, J., and Rothblat, G. (1992) *J. Lipid Res. 33*, 1699−1709.
4. Li, Q., Komaba, A., and Yokoyama, S. (1993) *Biochemistry 32*, 4597−4603.
5. Yancey, P., Bielicki, J., Johnson, W., Lund-Katz, S., Palgunachari, M., Anantharamaiah, G., Segrest, J., Phillips, M., and Rothblat, G. (1995) *Biochemistry 34*, 7955−7965.

6. Johnson, W., Mahlberg, F., Rothblat, G., and Phillips, M. (1991) *Biochim. Biophys. Acta 1085*, 273−298.
7. Saito, H., and Handa, T. (1999) *Curr. Top. Colloid Interface Sci. 3*, 19−33.
8. Wald, J., Krul, E., and Jonas, A. (1990) *J. Biol. Chem. 265*, 20037−20043.
9. Sparks, D., Davidson, W., Lund-Katz, S., and Phillips, M. (1993) *J. Biol. Chem. 268*, 23250−23257.
10. Saito, H., Minamida, T., Arimoto, I., Handa, T., and Miyajima, K. (1996) *J. Biol. Chem. 271*, 15515−15520.
11. Saito, H., Miyako, Y., Handa, T., and Miyajima, K. (1997) *J. Lipid Res. 38*, 287−294.
12. Yokoyama, S., Fukushima, D., Kupferberg, J. P., Kezdy, F, J., and Kaiser, E. T. (1980) *J. Biol. Chem. 255*, 7333−7339.
13. Saito, H., Tanaka, M., Okamura, E., Kimura, T., Nakahara, M., and Handa, T. (2001) *Langmuir 17*, 2528−2532.
14. Segrest, J., Jones, M., De Loof, H., Brouilette, C., Venkatachalapathi, Y., and Anantharamaiah, G. (1992) *J. Lipid Res. 33*, 141−166.
15. Mishra, V., and Palgunachari, M. (1996) *Biochemistry 35*, 11210−11220.
16. Mishra, V., Palgunachari, M., Datta, G., Phillips, M., Lund-Katz, S., Adeyeye, S., Segrest, J., and Anantharamaiah, G. (1998) *Biochemistry 37*, 10313−10324.
17. Polozov, I., Polozova, A., Molotkovsky, J., and Epand, R. (1997) *Biochim. Biophys. Acta 1328*, 125−139.
18. Clayton, A., and Sawyer, W. (2000) *Biophys. J. 79*, 1066−1073.
19. Datta, G., Chaddha, M., Hama, S., Navab, A., Fogelman, A., Garber, D. W., Mishra, V. K., Epand, R. M., Lund-Katz, S., Phillips, M. C., Segrest, J. P., and Anantharamaiah, G. M. (2001) *J. Lipid. Res. 42*, 1096−1104.
20. Anantharamaiah, G. M., Jones, J. L., Brouillette, C. G., Schmidt, C. F., Chung, B. H., Hughes, T. A., Bhown, A. S., and Segrest, J. P. (1985) *J. Biol. Chem. 260*, 10248−10255.
21. Mishra, V. K., Palgunachari, M. N., Segrest, J. P., and Anantharamaiah, G. M. (1994) *J. Biol. Chem. 269*, 7185−7191.
22. Molotkovsky, J., Dmitriev, P., Nikulina, L., and Bergelson, L. (1979) *Bioorgan. Khim. 5*, 588−594.
23. Bartlett, G. (1959) *J. Biol. Chem. 234*, 466−468.
24. Vladimirov, Yu. A., and Dobretsov, G. E. (1980) in *Fluorescent Probes in the Studies of Biological Membranes*, p 28, Nauka, Moscow.
25. Gazzara, J. A., Phillips, M. C., Lund-Katz, S., Palgunachari, M. N., Segrest, J. P., Anantharamaiah, G. M., and Snow, J. W. (1997) *J. Lipid Res. 38*, 2134−2146.
26. Bulychev, A. A., Verchoturov, V. N., and Gulaev, B. A. (1988) *Current Methods of Biophysical Studies*, Vyschaya shkola, Moscow.
27. Lakowicz, J. (1999) in *Principles of Fluorescent Spectroscopy*, 2nd ed., pp 267−269, Plenum Press, New York.
28. Gazzara, J. A., Phillips, M. C., Lund-Katz, S., Palgunachari, M. N., Segrest, J. P., Anantharamaiah, G. M., and Snow, J. W. (1997) *J. Lipid Res. 38*, 2147−2154.
29. Ladokhin, A., Selsted, M., and White, S. (1997) *Biophys. J. 72*, 794−805.
30. Ren, J., Lew, S., Wang, J., and London, E. (1999) *Biochemistry 38*, 5905−5912.
31. Chen, Y., and Barkley, M. (1998) *Biochemistry 37*, 9976−9982.
32. Johnson, D., and Yguerabide, J. (1985) *Biophys. J. 48*, 949−955.
33. Wolber, P., and Hudson, B. (1979) *Biophys. J. 28*, 197−210.
34. Clayton, A., and Sawyer, W. (1999) *Eur. Biophys. J. 28*, 133−141.
35. Hristova, K., Wimley, W., Mishra, V., Anantharamaiah, G., Segrest, J., and White, S. (1999) *J. Mol. Biol. 290*, 99−117.
36. Dobretsov, G., Petrov, V., and Mishiev, V. (1977) *Studia Biophys. 65*, 91−98.
37. Molotkovsky, J. G., Manevich, Y. M., Babak, V. I., and Bergelson, L. D. (1984) *Biochim. Biophys. Acta 778*, 281−288.
38. Huang, H. W. (2000) *Biochemistry 39*, 8347−8352.
39. Segrest, J., de Loof, H., Dohlman, J., Brouilette, C., and Anantharamaiah, G. (1990) *Proteins 8*, 103−117.
40. Tytler, E., Segrest, J., Epand, R. M., Nie, S., Epand, R. F., Mishra, V., Venkatachalapathi, Y., and Anantharamaiah, G. (1993) *J. Biol. Chem. 268*, 22112−22118.
41. Polozov, I., Polozova, A., Tytler, E., Anantharamaiah, G., Segrest, J., Wooley, G., and Epand, R. (1997) *Biochemistry 36*, 9237−9245.
42. Clayton, A. H. A., and Sawyer, W. H. (2000) *Biochim. Biophys. Acta 1467*, 124−130.
43. Dale, R., Eisinger, J., and Blumberg, W. (1979) *Biophys. J. 26*, 161−194.
44. Valeur, B., and Weber, G. (1977) *Photochem. Photobiol. 25*, 441−444.
45. Johansson, L., Molotkovsky, J., and Bergelson, L. (1990) *Chem. Phys. Lipids 53*, 185−189.
46. Ren, J., Lew, S., Wang, Z., and London, E. (1997) *Biochemistry 36*, 10213−10220.
47. Caffrey, M., and Feigenson, G. (1981) *Biochemistry 20*, 1949−1961.
48. Ivkov, V. G., and Berestovsky, G. N. (1981) in *Dynamic Structure of Lipid Bilayer*, Nauka, Moscow.
49. Sankaram, M., and Thompson, T. E. (1990) *Biochemistry 29*, 10675−10684.
50. Oldfield, E., Meadows, M., Rice, D., and Jacobs, R. (1978) *Biochemistry 17*, 2727−2740.
51. Gaus, K., Dean, R. T., Kritharides, L., and Jessup, W. (2001) *Biochemistry 40*, 13002−13014.
52. Monette, M., Van Calsteren, M., and Lafleur, M. (1993) *Biochim. Biophys. Acta 1149*, 319−328.
53. Nicol, F., Nir, S., and Szoka, F. (1996) *Biophys. J. 71*, 3288−3301.
54. Duzgunes, N., and Shavnin, S. (1992) *J. Membr. Biol. 128*, 71−80.
55. Pott, T., and Dufourc, E. (1995) *Biophys. J. 68*, 965−977.
56. Epand, R., Shai, Y., Segrest, J., and Anantharamaiah, G. (1995) *Biopolymers 37*, 319−338.
57. Bergeron, J., Frank, P., Scales, D., Meng, Q., Castro, G., and Marcel, Y. (1995) *J. Biol. Chem. 270*, 27429−27438.
58. Lecompte, M., Bras, A., Dousset, N., Portas, I., Salvayre, R., and Ayrault-Jarrier, M. (1998) *Biochemistry 37*, 16165−16171.
59. Rand, R., and Sengupta, S. (1972) *Biochim. Biophys. Acta 255*, 484−492.

BI011885+